Monthly Notices
of the
ROYAL ASTRONOMICAL SOCIETY

MNRAS **463,** 1740–1750 (2016)
Advance Access publication 2016 August 23

doi:10.1093/mnras/stw2109

Differential rotation, flares and coronae in A to M stars

L. A. Balona,[1]★ M. Švanda[2,3]★ and M. Karlický[3]★

[1]*South African Astronomical Observatory, PO Box 9, Observatory, Cape 2735, South Africa*
[2]*Astronomical Institute, Charles University in Prague, V Holešovičkách 2, CZ-18200 Praha, Czech Republic*
[3]*Astronomical Institute (v. v. i.), Czech Academy of Sciences, Fričova 298, CZ-25165 Ondřejov, Czech Republic*

Accepted 2016 August 19. Received 2016 August 6; in original form 2016 June 6

ABSTRACT

Kepler data are used to investigate flares in stars of all spectral types. There is a strong tendency across all spectral types for the most energetic flares to occur among the most rapidly rotating stars. Differential rotation could conceivably play an important role in enhancing flare energies. This idea was investigated, but no correlation could be found between rotational shear and the incidence of flares. Inspection of *Kepler* light curves shows that rotational modulation is very common over the whole spectral type range. Using the rotational light amplitude, the size distribution of star-spots was investigated. Our analysis suggests that stars with detectable flares have spots significantly larger than non-flare stars, indicating that flare energies are correlated with the size of the active region. Further evidence of the existence of spots on A stars is shown by the correlation between the photometric period and the projected rotational velocity. The existence of spots indicates the presence of magnetic fields, but the fact that A stars lack coronae implies that surface convection is a necessary condition for the formation of the corona.

Key words: stars: activity – stars: flare – stars: rotation – starspots.

1 INTRODUCTION

From the ground, flare stars are almost always associated with active M dwarfs (UV Ceti variables). In the optical, flares are most easily visible in the UV band. The star may suddenly brighten over a few minutes or seconds by as much as several magnitudes followed by a slower decay. The flare may be detectable across the electromagnetic spectrum from X-rays to radio waves. During a flare, the Balmer lines are in emission and a continuum resembling that of an A or B star, as well as the spectrum of ionized helium, makes an appearance (Kowalski et al. 2013). It is generally assumed that these are the stellar analogues of the rare 'white light' solar flares, though the energy release is several orders of magnitude larger. Flares from the Sun, observed as a star, cannot be detected from space, even with the most sensitive instruments currently available. Because of their high energies, the vast majority of stellar flares may be called 'superflares', but we will not use this term.

In spite of many decades of observations from the ground and from space, we are still far from understanding the process that gives rise to a flare. We know that a flare is a result of energy released during reconnection of magnetic field lines. This process occurs in the highly conducting plasma of the upper chromosphere or corona where magnetic energy is converted to kinetic energy, thermal energy, and particle acceleration (Shibata 1999). This results in the optical emission we recognize as a flare.

Convection, differential rotation and meridional circulation, which are all key ingredients in the current theory of the solar dynamo (Choudhuri, Schussler & Dikpati 1995; Küker & Stix 2001), play a central role in the generation of a flare. A small part of this mechanical energy is transferred to the magnetic field by twisting of field lines. It is this energy which is later released as a flare. While the Sun is the only body in which detailed flare processes can be examined, the roles of convection, rotation and differential rotation can only be explored by the study of stellar flares.

Space observations have detected stellar flares in the X-ray and extreme UV bands (Heise et al. 1975; Haisch et al. 1977), while radio emission from cool M dwarfs and active close binaries has been studied for a long time (Lovell 1963). Until recently, the study of stellar flares in the optical band has been almost entirely confined to ground-based observations of M dwarfs. It is only through the ultraprecise, low-noise optical photometry of the *Kepler* satellite that flares were finally detected in a wide range of main-sequence stars (Balona 2012; Maehara et al. 2012). Indeed, it may be that flares are an ubiquitous phenomenon among stars of all spectral types (Balona 2015). This discovery allows an investigation of the differing effects of convection, rotation, differential rotation and other stellar properties on the energy, frequency and duration of stellar flares. In this paper, we summarize and further explore how stellar flares observed by *Kepler* are affected by various global stellar properties.

★ E-mail: lab@saao.ac.za (LAB); michal@astronomie.cz (MS); marian.karlicky@asu.cas.cz (MK)

2 THE DATA

Before the launch of *Kepler*, the effective temperatures, surface gravities, metallicities and radii of each star in the *Kepler* field were estimated from ground-based multicolour photometry and listed in the *Kepler* Input Catalogue (KIC; Brown et al. 2011). These parameters have been updated from time to time, including the recent revision by Huber et al. (2014).

The *Kepler* spacecraft has obtained almost uninterrupted photometry over a 4-yr timespan of over 150 000 stars in the same field. *Kepler* light curves are available as uncorrected simple aperture photometry (SAP) and with pre-search data conditioning (PDC) in which instrumental effects are removed (Smith et al. 2012; Stumpe et al. 2012). The vast majority of stars were observed in long-cadence (LC) mode with exposure times of about 30 min. A few thousand stars were observed in short-cadence (SC) mode with exposure times of 1 min. These data are publicly available on the Barbara A. Mikulski Archive for Space Telescopes (MAST, archive.stsci.edu).

The failure of mechanical reaction wheels on board the spacecraft with the loss of fine pointing ability in 2013 May, forced the end of the original *Kepler* mission. Using the solar wind as an aid in stabilizing the pointing, the spacecraft has continued observations in fields along the ecliptic plane. While the pointing is still a problem, photometric precision approaching that of the original mission can be attained using correction algorithms. The new mission, *K2*, has continued obtaining valuable data, but unfortunately these data cannot be used to detect stellar flares with any degree of certainty.

This work therefore relies almost entirely on data from the original *Kepler* mission. All SC data as well as all LC data for stars with $T_{\rm eff} > 6500$ K were used. For the cooler stars, we included all LC data with *Kepler* magnitude $K_p < 12.5$ mag. The resulting list of over 20 000 stars was classified according to variability type in the manner of the *General Catalogue of Variable Stars* (Samus et al. 2009). This was done by visual inspection of the corrected and uncorrected light curves and periodograms together with knowledge of the approximate location of each star in the H-R diagram. Flares were detected in 755 stars which include stars previously recognized as flare stars in the literature, but also many new detections. These also include the 209 flare stars observed in SC mode and described by Balona (2015). Because of the poor time resolution, only flares of long duration can be detected in LC mode.

3 WHAT IS KNOWN

It is appropriate at this stage to summarize what we already know about flare stars.

Flares appear to occur in main-sequence stars of all spectral types (Balona 2012; Maehara et al. 2012). Although flares in B stars have not yet been identified due to the very small number of B stars in the *Kepler* field, it seems likely that they should exist since there is no fundamental difference in the atmospheric structure of A and B stars. The O stars and the early B stars have strong radiatively driven stellar winds. Although it is generally supposed that the X-ray emission from these stars is a result of shocks in the stellar wind, the possibility that X-ray emission could be a result of magnetic reconnection of field lines threading the stellar wind should perhaps also be considered.

A flare is detected in the *Kepler* data by its characteristic shape, provided the signal-to-noise (S/N) ratio is sufficiently high. This means that the more luminous the star, the more energetic the flare needs to be in order to be detected. The higher the flare energy, the less frequent the occurrence of the flare. It is thus not surprising that the number of flare stars relative to non-flare has been found to decrease by a factor of 4 between types K-M and type A (Balona 2015). It seems probable, therefore, that flares are common among all main-sequence stars. When we talk of 'non-flare' stars, we merely mean stars where the flare energies are too low to be detected.

From the above reasoning, one expects that the energies, E, of detected flares should increase with stellar luminosity, $L/{\rm L}_\odot$, which is indeed the case (Balona 2015). If the distribution of flare energy is the same for stars of all spectral types, we expect to see as many high-energy flares in cool stars as in hot stars, but this is not the case. The very high flare energies seen in F and A stars are not seen in K and M stars. Such flares should, of course, be the easiest to detect among the cool stars. In other words, the increase of flare energy with luminosity is a real effect.

There is a striking correlation between the incidence of flares and the stellar rotation rate. It is found that flare stars rotate at a considerably higher rate than non-flare stars (Balona 2015). This shows that the higher the rotation rate, the more energetic the flare. The rotation rate of solar-like stars declines with age owing to the loss of angular momentum in the magnetically coupled stellar wind. It is also supposed that the stellar dynamo becomes less efficient as the rotation rate declines. This in turn leads to a weaker magnetic field, fewer active regions and less flaring (Noyes et al. 1984). The effect of rotation on flare energy can thus be ascribed to an age effect. However, this reasoning does not apply to A stars since the very thin subsurface convection zones which are present (Kallinger & Matthews 2010) are not sufficient to drive a dynamo. Furthermore, A stars do not possess a hot corona nor an effective stellar wind. However, the number of flare A stars are too few to determine whether rotation plays a role in flare energy.

The flaring rate in *Kepler* flare stars has been studied in some detail. Maehara et al. (2012) studied only main-sequence G stars and found that the frequency distribution function (i.e. flare rate, $\mathrm{d}N/\mathrm{d}E$ as a function of flare energy, E) is similar to that in the Sun. This was confirmed by Shibayama et al. (2013) who found $\mathrm{d}N/\mathrm{d}E \approx E^{-2}$. Also, the frequency distribution function increases with increasing rotation rate (Maehara et al. 2012; Shibayama et al. 2013; Candelaresi et al. 2014). In other words, the flaring rate for a given flare energy is higher in a rapidly rotating star than in a slowly rotating G star. The flaring rate is also found to decrease with increasing effective temperature (Maehara et al. 2012; Shibayama et al. 2013).

Shibayama et al. (2013) suggest that flare stars have extremely large star-spots with sizes typically about 10 times larger than that of the largest sunspot. Balona (2015) compared the median light amplitudes in *Kepler* stars classified as rotational variables for flare and non-flare stars. There does indeed appear to be a trend for flare stars of a particular spectral type to have larger median light amplitudes than non-flare stars. This can be interpreted to mean that larger flare energies are correlated with larger star-spots.

4 ROTATION

Here we study the effect of rotation, not on the flaring rate, but on the flare energy. Rotation periods in *Kepler* stars can often be deduced by the presence of rotational light modulation as a result of star-spots. Several catalogues of rotation period exist (Balona 2013; McQuillan, Mazeh & Aigrain 2013, 2014; Nielsen et al. 2013; Reinhold, Reiners & Basri 2013). We used, in the first instance, the rotation periods of flare stars given by Balona (2015) derived from

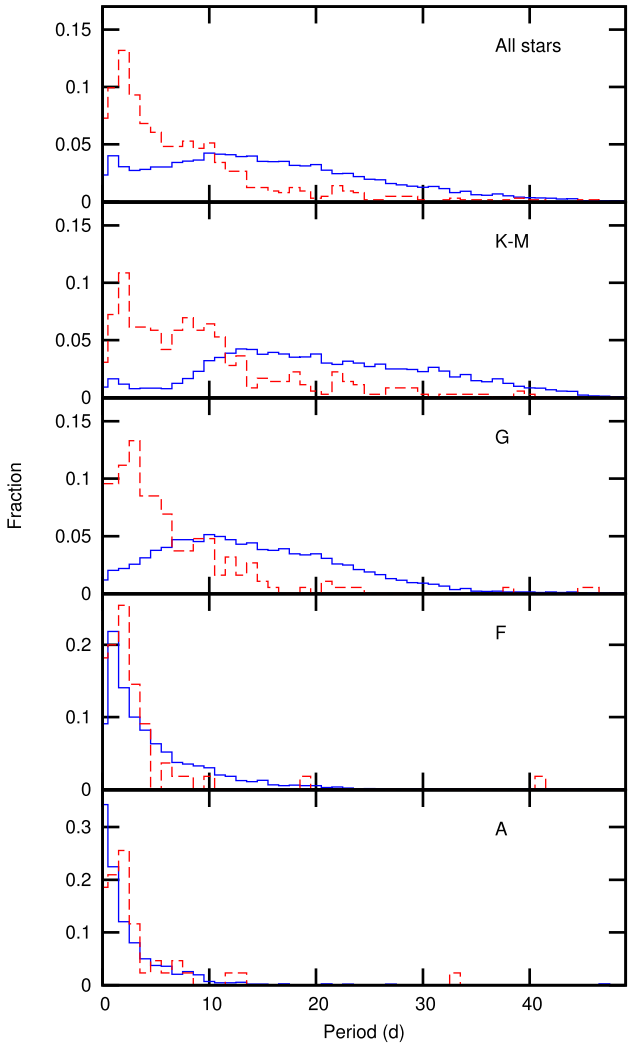

Figure 1. Distribution of rotation periods of stars with the given spectral types. The solid (blue) histogram is for all stars; the dashed (red) histogram is for flare stars.

Kepler SC data. These were supplemented by the rotation periods of A stars observed in LC mode (Balona 2013). Rotation periods, $P_{\rm rot}$, for most of the other stars could be found in the other catalogues mentioned above. For the most part, the periods in these catalogues agree very well, although in a few cases it is clear that the first harmonic of the rotation period, and not $P_{\rm rot}$ itself, is listed. The adopted value of $P_{\rm rot}$ for a given star is the average value appearing in these catalogues. Our final list contains 645 flare stars with known rotation periods.

We wish to compare the rotation periods of flare stars with the rotation periods of all main-sequence stars (flare and non-flare) within restricted effective temperature (spectral type) ranges. By restricting the stars to a fairly narrow $T_{\rm eff}$ range, i.e. luminosity range, we are essentially detecting flares above a minimum energy level. Our aim is to discover the effect of rotation on flare energy. If such an effect does not exist, we should find no difference in the distributions between flare and non-flare stars of a given spectral type. Balona (2015) found that flare stars tend to have significantly shorter rotation periods. This is shown in Fig. 1. Table 1 lists the mean rotational periods for all stars and for flare stars.

What we have shown is different from the correlation between flaring frequency and rotation (Maehara et al. 2012; Notsu et al. 2013; Shibayama et al. 2013; Candelaresi et al. 2014). Flaring frequency is not considered here, but only the simple occurrence of one or more flares above a certain threshold energy level which varies with spectral type. In other words, what has been demonstrated is that higher rotation rate implies, in general, a higher flare energy. This may be explained as an age effect as described above.

Table 1. The mean rotation period, $P_{\rm rot}$ (in days) and the number of stars, N, used to construct the period distributions for all stars and for flare stars of a particular spectral type.

	All stars		Flare stars	
Sp.Ty.	$P_{\rm rot}$	N	$P_{\rm rot}$	N
A	3.16 ± 0.14	1121	3.96 ± 0.85	43
F	5.32 ± 0.07	6196	3.75 ± 0.81	55
G	14.68 ± 0.04	40 023	6.68 ± 0.49	189
K–M	21.19 ± 0.07	23 516	9.72 ± 0.42	359

In order to test this idea further, we require flare stars with as wide a range of rotation periods as possible. It is difficult to find stars with very small rotation periods among stars of solar type. It would be important to include more F, and particularly A stars, which generally rotate with much shorter periods than cooler stars. Of course, these stars need to have detectable rotational modulation (star-spots) in order to measure their rotation periods.

5 DIFFERENTIAL ROTATION

Recently, Balona & Abedigamba (2016) found that differential rotation on the main sequence varies with effective temperature and rotation rate. The absolute rotational shear, $\Delta\Omega$, which is the difference between the rotation rate at the equator and the poles, reaches a maximum for F-type stars, decreasing somewhat for A stars. The possibility exists that it is not so much the rotation rate, Ω, that is a factor in inducing flares, but differential shear, $\Delta\Omega$ which, as we have seen, also depends on Ω. A large rotational shear may assist in twisting of magnetic field lines or may feed into the flare-generating process in some other way. The role of $\Delta\Omega$ in flare production can be tested by examining whether or not it is significantly different between flare and non-flare stars.

A lower bound of the absolute rotational shear can be estimated by measuring the rotational frequency spread, $\delta\omega$, in a time-frequency diagram (Balona & Abedigamba 2016). For this purpose, we were able to measure $\delta\omega$ in 617 flare stars with known rotation periods. The mean value of $\delta\omega$ is proportional to $\Delta\Omega$. As in Balona & Abedigamba (2016), we fixed the factor of proportionality by assuming that stars with approximately the same $T_{\rm eff}$ and Ω as the Sun will have the same value of $\Delta\Omega$ as the Sun. Individual estimates of $\Delta\Omega$ for flare and non-flare stars are shown in Fig. 2. It should be noted that $\Delta\Omega$ depends both on $T_{\rm eff}$ and Ω, and that Fig. 2 does not separate the dependences.

In order to compare the value of $\Delta\Omega$ for flare and non-flare stars, we need to ensure that its dependence on both $T_{\rm eff}$ and Ω is taken into account. This can be done by comparing stars with a fixed rotation period, $P_{\rm rot}$ in a diagram showing $\Delta\Omega$ as a function of $T_{\rm eff}$ or stars with fixed $T_{\rm eff}$ in a diagram showing $\Delta\Omega$ as a function of $\Omega = 2\pi/P_{\rm rot}$. Such a comparison is shown in Figs 3 and 4. Owing to the finite number of stars, these diagrams were constructed using non-zero, but reasonably small, ranges of $P_{\rm rot}$ and $T_{\rm eff}$. It is evident that there is no significant difference in $\Delta\Omega$ between flare and non-flare stars. In other words, the flare energy does not seem to be correlated in any way with the differential rotation shear.

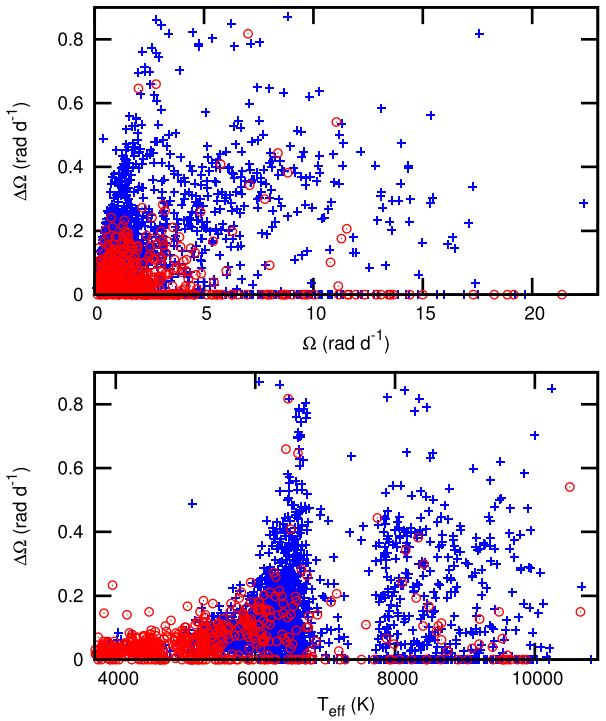

Figure 2. Individual measurements of normalized differential rotation shear, $\Delta\Omega$, as a function of angular rotation rate (top panel) and effective temperature (bottom panel) for non-flare stars (blue crosses) and flare stars (red open circles).

6 STAR-SPOTS

The light curve due to a rotating star with one or more spots is fairly easy to recognize. It consists of a sinusoidal variation with beats and slight changes in frequency in the low-frequency range. There are two types of pulsating star which can produce similar light curves: the F-type γ Dor variables and the mid- to late-B SPB variables. The δ Sct stars also vary with multiple low frequencies, but these are easily recognized by the high frequencies (typically larger than 5 d^{-1}). Inspection of the light curve and periodogram together with knowledge of the approximate location of the star in the H-R diagram allows a star to be classified as a rotational variable. No δ Sct stars are included in this analysis, but it is possible that some γ Dor stars may have been classified rotational variables.

Even a brief inspection of *Kepler* light curves suggests that rotational variables are quite common. A measure of the fraction of rotational variables in each spectral type can be estimated from our sample of over 20 000 stars. The distribution is shown in Fig. 5. It can be seen that nearly half the stars of all spectral types may be rotational variables. Caution is required for the B stars because of small numbers and possible confusion with SPB variables. Nevertheless, the fraction of rotational variables among the B stars is probably quite high, judging from a study of B stars in the K2 mission (Balona 2016).

It is to be expected that the most energetic flares should be associated with the largest active regions. We cannot directly detect active regions in a star, but we can make the assumption that the amplitude of the light variation due to rotational modulation is related to the size of a star-spot and hence a measure of the size of the active region. We do not have information concerning the typical emergent flux from a spot in the *Kepler* passband or the flux

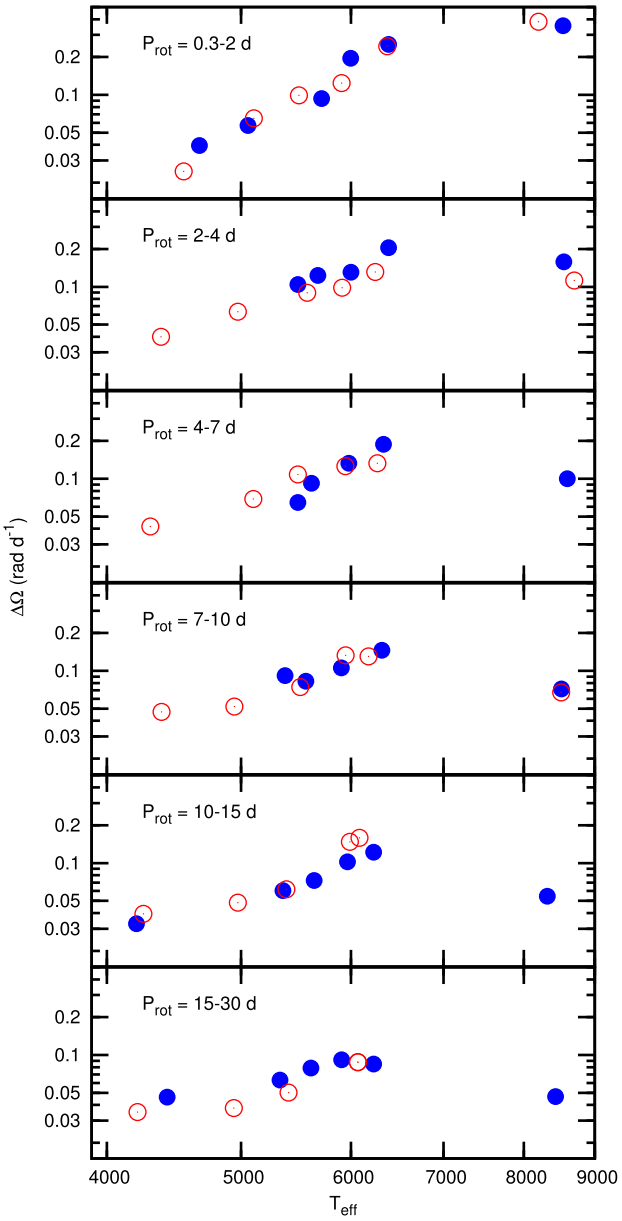

Figure 3. The normalized differential rotation shear, $\Delta\Omega$, as a function of effective temperature for the indicated ranges of rotation period. The filled (blue) circles are non-flare stars while the open (red) circles are flare stars.

relative to the surrounding photosphere. Furthermore, the flux in the direction of the observer depends on the limb darkening law, the latitude of the spot and the inclination of the rotation axis to the line of sight.

In view of these unknowns, the best that can be done is to assume that a spot is circular, completely dark and randomly distributed in latitude. In that case, the amplitude of the light variation at the period of rotation is approximately the ratio of the star-spot area relative to the area of the stellar hemisphere. If we know the approximate stellar radius, we can obtain a rough estimate of the absolute area of the star-spot from the light amplitude at the rotation period.

To obtain these estimates, the group of stars used for a previous study of differential rotation (Balona & Abedigamba 2016) was selected. The amplitude and period of a rotational variable both vary with time as spots change in size and migrate in latitude, leading

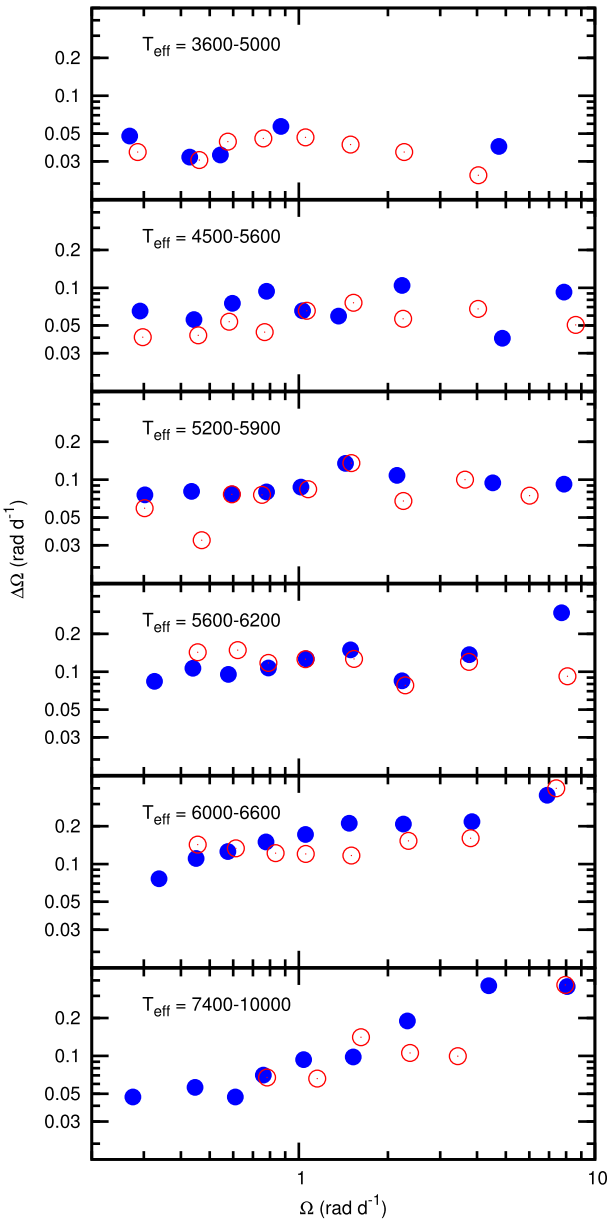

Figure 4. The variation of $\Delta\Omega$ as a function of angular rotation frequency for the indicated ranges of effective temperature. The filled (blue) circles are non-flare stars while the open (red) circles are flare stars.

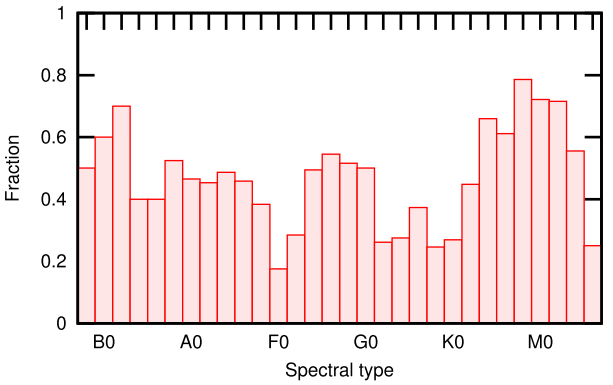

Figure 5. The fraction of stars classified as rotational variables by visual inspection of *Kepler* light curves and periodograms.

Table 2. The mean logarithm of the star-spot area, A, measured in MSH, and the number of stars, N, in non-flare and flare stars of different spectral types.

	All stars		Flare stars	
Sp.Ty.	$\log A$	N	$\log A$	N
A	2.54 ± 0.03	493	3.13 ± 0.16	43
F	2.54 ± 0.02	1124	3.19 ± 0.07	79
G	2.78 ± 0.03	567	3.57 ± 0.05	184
K–M	2.52 ± 0.18	30	3.14 ± 0.04	310

to a broadening of the peak in the periodogram. It is not really possible to follow these changes for a particular spot, but one may take the amplitude calculated by the Lomb–Scargle periodogram at the rotational frequency as a reasonable estimate of the amplitude produced by a typical spot (or spot group). The stellar radius was estimated using the revised effective temperature, surface gravity and metallicity in the catalogue of Huber et al. (2014) and the relationship in Torres, Andersen & Giménez (2010). Given the stellar radius in solar units, $R/\mathrm{R}_\odot$, the surface area of a spot, A, is given by $A = (R/\mathrm{R}_\odot)^2 A_V \times 10^{+6}$, where A_V is the fractional light amplitude and A is measured in micro solar hemispheres (MSH). This is the standard unit in measuring the size of active regions on the Sun.

Since the spot is unlikely to be completely dark, the estimated areas are lower limits. Polar spots are also not detectable as they do not give rise to periodic light modulation. Moreover, if the temperature difference between the spot and the surrounding photosphere is about the same and independent of effective temperature, the true spot size will be greater in hotter stars due to the decreased flux contrast. The average value of $\log A$ and its standard deviation for different spectral types is given in Table 2, where A is expressed in MSH. The distribution of spot sizes is shown in Fig. 6. It is evident from Table 2 and Fig. 6 that the active regions in flare stars are systematically larger than those in non-flare stars. Notice that the distribution of star-spot areas is approximately lognormal, as it is in the Sun.

For comparison, we note that the largest umbral areas on the Sun typically do not exceed 100 MSH (Bogdan et al. 1988), the largest sunspot ever observed (1947 April) had a total area of 4900 MSH including the penumbra (Hoge 1947). The umbral area would be about 1000 MSH. From Table 2, the typical size of a star-spot is about 400 MSH in non-flare stars and about 1500 MSH in flare stars. Interestingly, star-spot sizes reach a maximum for G stars and decrease by a factor of 3 for F and A stars. This does not support the suggestion that the increase in flare energy in F and A stars relative to the cooler stars is a result of the larger volume available for the active region (Balona 2015). Of course, we have ignored the possible decreasing spot contrast for the hotter stars which will lead to an underestimate of star-spot umbral sizes for F and A stars.

7 STAR-SPOTS ON A AND B STARS

In the above discussion, we have assumed that star-spots do exist in A stars despite the fact that current opinion holds that the subsurface convection zones in these stars (Kallinger & Matthews 2010) are too thin for the dynamo effect to operate. The evidence for star-spots on A stars is set out in Balona (2013) where it is shown that the distribution of rotation periods derived from *Kepler* photometry is the same as the distribution of rotational periods derived from spectroscopic measurements of the projected rotational velocities, $v \sin i$, for

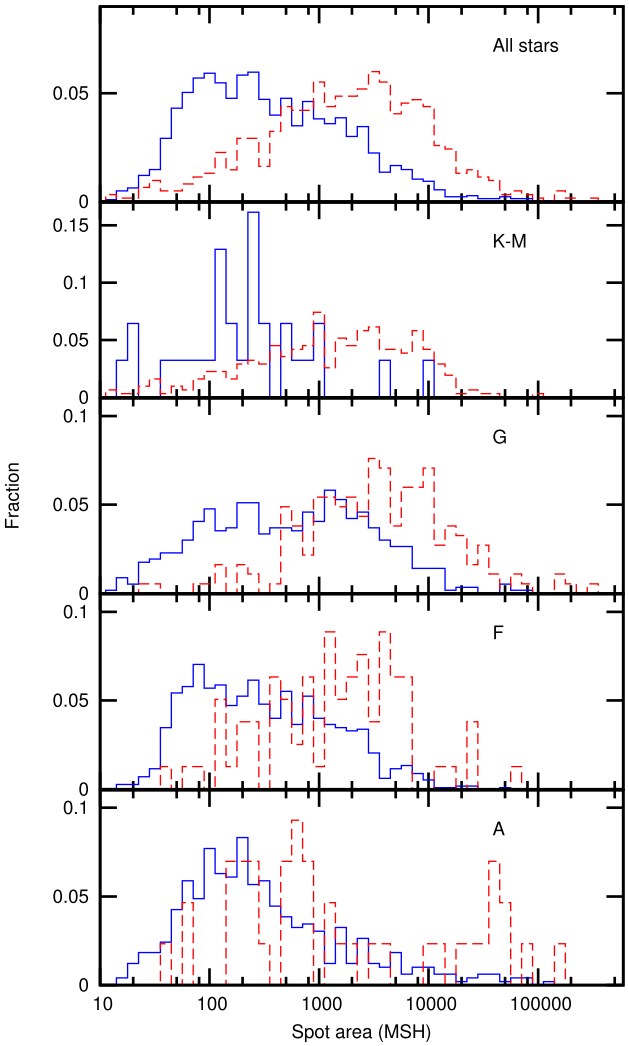

Figure 6. The distribution of approximate star-spot areas (in MSH) for non-flare stars (solid blue histogram) and for flare stars (dashed red histogram) in different spectral type ranges.

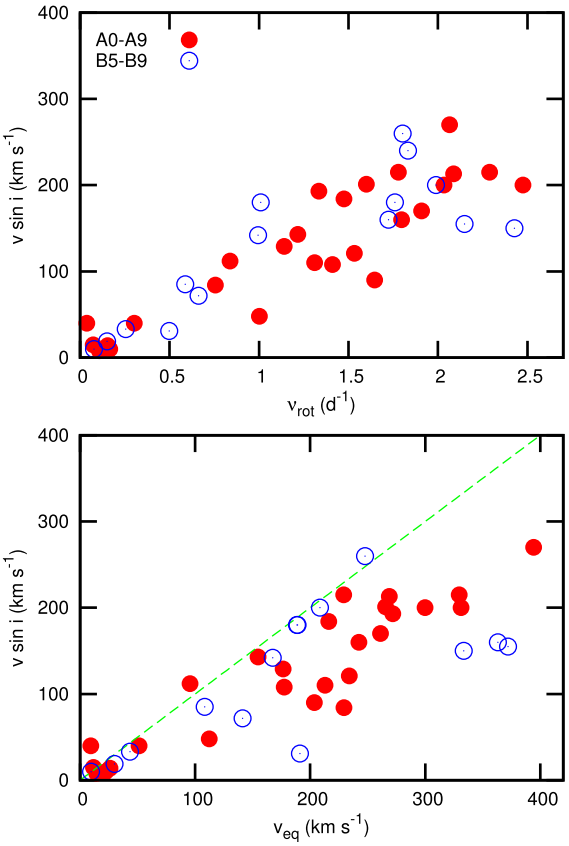

Figure 7. Top panel: projected rotational velocity, $v \sin i$, as a function of photometric frequency, $\nu_{\rm rot}$. Bottom panel, the projected rotational velocity as a function of equatorial rotational velocity, $v_{\rm eq}$, derived from $\nu_{\rm rot}$ and the stellar radius from the KIC. The line has unit slope. A stars and mid- to late-B stars are shown by different symbols.

main-sequence A stars in the field. At that time very few measurements of $v \sin i$ were available for *Kepler* A stars. Since then, the number of A stars with known $v \sin i$ has grown to 28, while the number of mid- to late B stars is 15. These numbers include a few stars observed by the K2 mission.

In Fig. 7, we show in the top panel the relationship between $v \sin i$ and the rotation period. There is a clear correlation, indicating that the photometric period is indeed the rotation period. In the bottom panel we deduce the equatorial rotational velocity, $v_{\rm eq}$, from the photometric period and an estimate of the radius obtained from the effective temperatures and surface gravities. The equatorial velocity should, of course, be larger than or equal to $v \sin i$. This means that the points in this graph should lie below the straight line. They do, which would not be the case if the light-curve periods were different from the rotation periods.

There is an indication that the relationship seen in A stars extends into the late- and mid-B stars, as might be expected. It is safe to assume that these stars, too, have active regions and might be expected to flare. It becomes increasingly difficult to detect flares in such luminous stars unless the flare energy continues to increase with luminosity.

8 CORONAE

The problem of what heats the solar corona is still unresolved after almost a century (De Moortel & Browning 2015). One class of models assumes that flares play a significant role (Parker 1988). Energetic considerations convincingly show that the energy released by large solar flares is not sufficient to cover radiative losses from the corona. The evidence favours a continuous source rather than an impulsive source of heating. Another idea is that heating is due to a large number of small-scale flares (nanoflares) with energies 10^{23}–10^{24} erg. The fact that A stars have flares, but no coronae, suggests that there is more to coronal heating than energy input from flares or nanoflares.

Stellar coronae can be detected from lines of highly ionized elements detected in X-ray spectra (Güdel & Nazé 2009). From these observations, it is known that coronae are ubiquitous among cool stars. Stellar coronae also emit in the X-ray continuum where it is found that the X-ray flux is related to the coronal temperature (Johnstone & Güdel 2015). X-ray emission in cool stars is also strongly correlated with rotation rate (Pallavicini et al. 1981; Wright et al. 2011). This is interpreted as a correlation between stellar activity and stellar rotation. Because the magnetized stellar wind is also believed to be driven by the stellar dynamo, rotation and magnetic activity effectively operate in a feedback loop with rotation, stellar activity and the stellar wind decreasing with age.

Because the depth of the convection zone decreases sharply for stars earlier than type F, it is thought that stellar coronae are

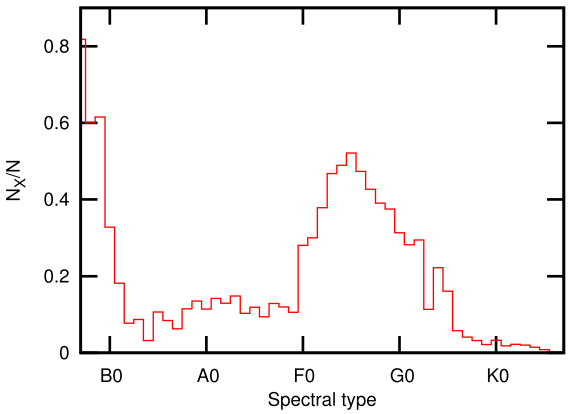

Figure 8. Relative numbers of X-ray active stars N_X/N in the Bright Star Catalogue as a function of spectral type. Note the X-ray 'hole' between B1 and F0.

essentially absent in stars hotter than about mid-A. Neff & Simon (2008) obtained far-UV spectra of 14 A stars, of which 11 exhibit detectable O VI emission which suggests the presence of a high-temperature chromosphere or corona. However, they conclude that emission from the higher temperature stars is more likely due to very active late-type dwarf binary companions.

The relative number of stars, N_X/N, in each spectral type which have been detected by X-rays is shown in Fig. 8. These data were compiled from Berghoefer et al. (1997) who list all O and B stars in the Yale Bright Star Catalogue which are detected by the *ROSAT* all-sky X-ray survey. Similarly, Huensch, Schmitt & Voges (1998) lists A, F, G and K stars in the Yale Bright Star Catalogue detected by *ROSAT*. This diagram was first compiled by Schröder & Schmitt (2007).

The drop in X-ray detections for cool stars is merely a result of the small number of stars (there are no bright M dwarfs) and does not reflect a lack of coronae. The X-ray emission in early B stars is thought to be a result of shocks in the radiatively driven stellar winds. What is noticeable is the low level of X-ray detections between B1 and A9, indicating that coronae are absent in these stars. Note that while the X-ray activity for B1–A9 stars is small, it is not zero. It is generally thought that this residual activity arises from unseen cool companions (De Rosa et al. 2011). This may well be the case, but the possibility that part of the activity may be due to stochastic X-ray emission from flares should not be excluded.

The above scenario agrees with the generally accepted view that only stars with convective envelopes can generate magnetic fields, which explains why the B1–A9 stars do not have coronae. However, if A stars do have magnetic fields, as suggested by star-spots and flares, this explanation cannot be complete. The observations indicate that only stars with convective envelopes possess coronae. Both mainstream competing hypotheses to explain the coronal heating, either by nanoflares (Parker 1988) or by magnetohydrodynamic waves (Alfvén 1947), require processes in the magnetic field to transport the energy to heat up the upper layers of the solar atmosphere. Convection is a likely source of energy. It may be that on stars without convective envelopes neither mechanism delivers enough energy to the upper atmosphere to compensate for radiative losses. These mechanisms may only be sufficiently effective in stars with significant near-surface convection. Note that in the models of Spruit (1999, 2002) and Maeder & Meynet (2004) convection is not required to produce a magnetic field. Thus, it is conceivable that flares and spots may occur in the absence of surface convection.

Table 3. Statistics of 209 flare stars observed in SC mode. The typical effective temperature, $\langle T_{\rm eff}\rangle$, stellar mass, $\langle M/{\rm M}_\odot\rangle$, and radius, $\langle R/{\rm R}_\odot\rangle$ for stars of the given spectral type are listed. The number of flare stars in each spectral type, the total number flares and the average number per star is given. The mean and median energies, E (erg), power (energy per unit time), W (erg s^{-1}), and mean and median durations, δt (s), are shown.

Parameter	A	F	G	K–M
$\langle T_{\rm eff}\rangle$	8570	6360	5490	4200
$\langle M/{\rm M}_\odot\rangle$	2.29	1.41	1.00	0.61
$\langle R/{\rm R}_\odot\rangle$	3.28	2.38	1.51	0.76
No. of stars	12	41	98	56
No. of flares	28	172	1650	1251
Flares/star	2.33	4.20	16.83	22.34
$E_{\rm mean}$	1.8×10^{36}	2.5×10^{35}	3.2×10^{35}	3.7×10^{35}
$E_{\rm median}$	3.5×10^{35}	4.9×10^{34}	3.1×10^{34}	1.1×10^{34}
$W_{\rm mean}$	5.6×10^{32}	4.8×10^{31}	4.3×10^{31}	3.2×10^{31}
$W_{\rm median}$	1.2×10^{32}	2.1×10^{31}	1.2×10^{31}	7.1×10^{30}
$\delta t_{\rm mean}$	3000	2900	4100	2400
$\delta t_{\rm median}$	2100	2200	2500	1600

9 FLARING RATE

One of the questions that needs to be asked is whether the flaring rate distribution as a function of flare energy differs for different spectral types. For this purpose, we use the 3140 flare events in 209 stars detected in the *Kepler* SC data (Balona 2015). These flares are well resolved in time. The use of LC data excludes short-lived flares and underestimates the energy of flares with durations shorter than a few hours. We divide the set of 209 stars into four spectral classes using the effective temperatures listed in the KIC. Table 3 summarizes the flare properties as a function of spectral type. The mean stellar parameters were weighted according to the number of flares in a star in order to be more representative of flare stars. Since the distribution of flare energy and mean power is highly asymmetrical, both the mean and median values are listed. As can be seen, the largest flare energy and power is to be found among the A stars.

Solar flares are believed to be the consequence magnetic reconnection of field lines in the corona, usually above a large active region. Studies show that the energy of a solar flare varies over a wide range (Crosby, Aschwanden & Dennis 1993; Shimizu 1995; Aschwanden et al. 2000). Magnetic reconnection is essentially a process with a 'self-organized criticality' (Aschwanden et al. 2016). The idea of self-organized criticality is commonly illustrated conceptually with avalanches in a pile of grains. The grains are dropped on to a pile one by one, and the pile ultimately reaches a stationary 'critical' state in which its slope fluctuates about a constant angle of repose, with each new grain being capable of inducing an avalanche on any of the relevant size scales. The energy distribution of solar flares can be described by a power law of the form $\mathrm{d}N(E)/\mathrm{d}E \propto E^{\alpha}$, where $N(E)$ is the number of flares at a given energy E and α is the power-law index. Various studies have shown that for solar flares $\alpha \approx -1.7$. For solar-like G stars $\alpha \approx -2$ (Shibayama et al. 2013; Maehara et al. 2016).

We determined the value of α in stars of different spectral types using the SC data. The resulting distributions are shown in Fig. 9. A power law was fitted to the part of the distribution beyond the maximum, i.e. for $E > 10^{34}$ erg. The cut-off at low energies is due to the fact that a flare needs to have a certain minimum energy (which varies with stellar luminosity) in order to be detected. In the *Kepler* data, one can only detect a flare if its relative amplitude is approximately 10^{-4}, setting a lower limit of about $10^{-4}L$ where

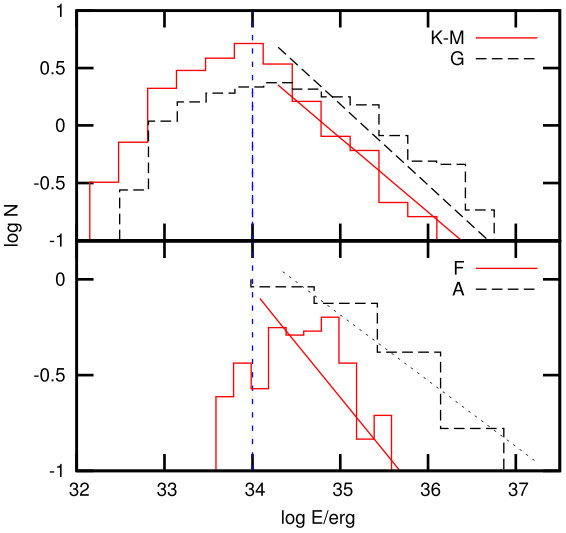

Figure 9. The distribution of mean flare energies for various spectral types. Power-law fits to energies higher than indicated by the vertical line are shown.

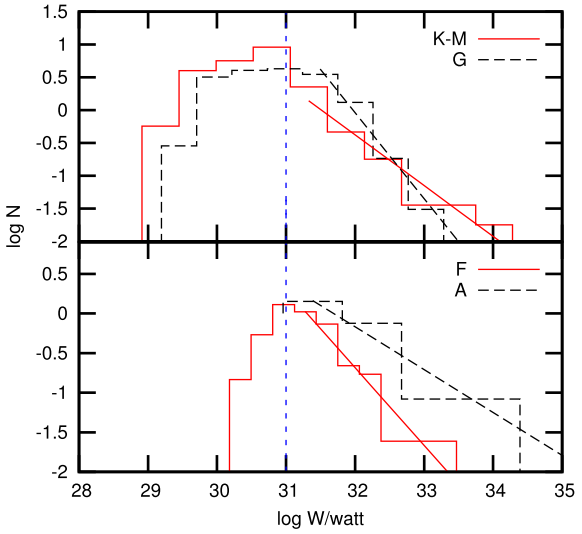

Figure 10. The distribution of mean flare power for various spectral types. Power-law fits to powers higher than indicated by the vertical line are shown.

L is the luminous energy of the star. L is about 100 times smaller for M stars than for A stars, so the lower detectable energy limit should increase from M to A stars. We determined the following power indices α: -1.65 for K–M stars, -1.70 for G stars, -1.56 for F stars and -1.34 for A stars.

We performed Kolmogorov–Smirnov tests to investigate whether the observed distribution functions of flare energies differ according to spectral type. The tests were applied to the part of histogram, where the flare energy exceeds 10^{35} erg to avoid the selection effect at low energies. The empirical distribution functions for A, F, and K–M stars were compared to the distribution in G stars. The null hypothesis was that the difference in the flare distribution function for various spectral types was due to chance. It turned out that the distribution function for A and F stars was different from G stars at the 95 per cent level, whereas no significant difference could be found between K-M and G stars.

A similar test can be performed for the mean power of flares (see Fig. 10). Kolmogorov–Smirnov tests show that the power distribution function for A stars differs from that of G stars at the 95 per cent confidence level, whereas no significant difference can be found for other spectral types. These tests depend on how the choice of minimum energy is made. Due to the small number of A stars, we cannot clearly state that there is a significant difference in the flare energy or power distribution between the A stars and other spectral types. Given the existing data, the evidence indicates that the power-law index is the same in all stars, irrespective of spectral type.

10 FLARE DURATIONS

Various models of solar flares assume that the total duration of a flare, δt, is a reasonable estimate for the time over which magnetic reconnection takes place. The reconnection time, $\tau_{\rm rec}$, may be estimated from the reconnection speed. We can assume that the reconnection speed is approximately proportional to the Alfvén speed, $v_{\rm A}$, in which case the flare duration can be approximated by $\delta t \sim \tau_{\rm rec} \propto (L/v_{\rm A})/M_{\rm A}$, where L is the length-scale of the magnetic field (flare loop length) which is dissipated during the reconnection event, and $M_{\rm A}$ is a non-dimensional reconnection rate which lies in the range 0.1–0.01 for fast reconnection in solar flares (Shibata & Magara 2011).

The total energy dissipated during a flare event may be estimated from $E \sim fE_{\rm m} \propto fB^2L^3$, where $E_{\rm m}$ is the total magnetic energy of the dissipated magnetic field and f is the estimated fraction of this energy released during the flare. By assuming that $v_{\rm A}$ and B are similar for the same type of stars, one obtains a scaling law of the form $\delta t \propto E^{1/3}$.

This scaling law, $\delta t \propto E^{\beta}$, can be tested using the SC data. It is found that for A stars $\beta = 0.26 \pm 0.06$ (correlation coefficient $\rho = 0.64$); for F stars $\beta = 0.38 \pm 0.03$ ($\rho = 0.72$); for G stars $\beta = 0.33 \pm 0.01$ ($\rho = 0.74$); and for K–M stars $\beta = 0.28 \pm 0.01$ ($\rho = 0.60$). We did not consider the errors in both flare duration and flare energy, but it is clear that β is close to the expected value of 1/3 for all spectral types.

The distribution of flare energies and flare durations suggest that stellar flares behave in a similar way to solar flares, which indicates that the same mechanism, magnetic reconnection, is at work in all cases.

11 FLARES IN A STARS

Because A stars have radiative envelopes, the discovery of flares in the *Kepler* photometry (Balona 2012) was unexpected. Flares were detected by simple visual inspection of the raw *Kepler* light curves. Flares are seen in both the SC (1-min exposures) and LC (30-min exposures) light curves. Of course, the time resolution and amplitudes of the flare is much reduced in the LC data, even though the S/N ratio is higher.

Examples of flares seen in A, F and G stars seen in the SC data are shown in Fig. 11. Examination of the actual pixel data of the brightest A-type flare stars show that the signal occurs in each pixel of the star image. The possibility that these are simply noise signals is very unlikely since no other star in the same CCD field of view shows the same signal at the same time. Of course, light curves from flare stars are never repeatable, but it would not be correct to dismiss such evidence simply because it does not fit in with current ideas. As can be seen from Fig. 11, flares on A stars have the same appearance as flares on cooler stars.

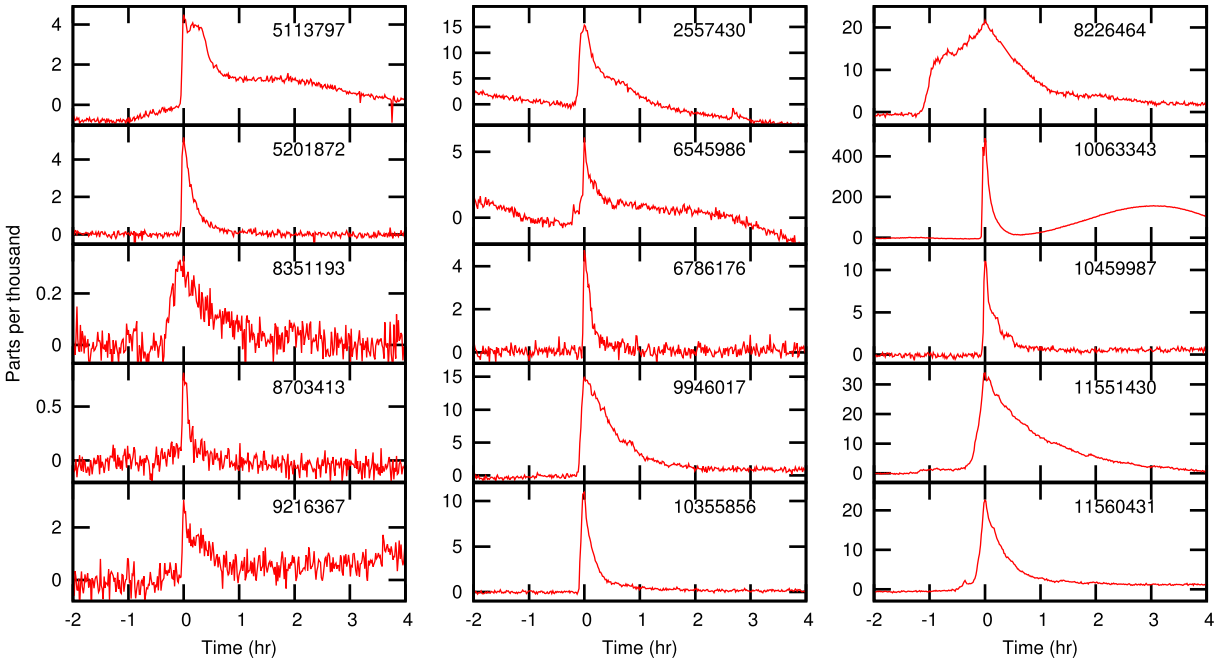

Figure 11. Examples of flares in stars of different spectral types detected in the SC *Kepler* data. Left-hand panel: A stars; middle panel: F stars; right-hand panel: G stars. The labels are KIC numbers.

Balona (2013) announced further detections and analyses of these flares. In Balona (2015), it is argued that the relative number of A stars which flare is probably the same as in cooler stars. It is just the higher luminosity of the A stars which prevent the detection of all except the most energetic flares. It is quite natural to suppose that these flares are not on the A star itself, but perhaps on a late-type companion. This idea seems very unlikely. A stars are about 100 times more luminous than K dwarfs. As a result, a typical flare on a K dwarf companion will have an amplitude one hundred times smaller than on an isolated K dwarf. The average maximum amplitude of flares in *Kepler* K stars is well known and about the same as the average maximum amplitude of flares in A stars (Balona 2012, 2013, 2015). If one insists that these flares are all on cool dwarfs, an explanation is required as to why such flares are 100 times more energetic than in single cool dwarfs. On the other hand, if the companion is an F or G star, the brightness of the companion would distort the colour so that the composite star would no longer be classified as a hot A star. At least 10 A-type flare stars have spectral classifications ranging between B8 and A3 (see table 2 of Balona 2013).

In spite of this argument, it is still important to obtain spectra of these flare stars and to search for possible cool companions. So far, no such observations have been done. The stars are relatively faint and high-resolution observations are necessary, requiring a large telescope. Even if no cool companion were to be detected, it can always be argued that the cool star is just below the detection limit. Against such an argument, no amount of reasoning is sufficient. However, the onus is on the skeptic to prove that flares on the supposed cool companion are typically 50–100 times larger than on isolated field K dwarfs when in orbit around an A star, as discussed above. Of course, the detection of star-spots on A stars was also a surprise. If one accepts that star-spots are present, as the observations clearly indicate they do, it is no longer so difficult to accept that flares are possible on A stars since all the relevant conditions for flaring are already present.

The *Kepler* observations are by no means the first time that flares have been detected on A stars. Schaefer (1989) reported cases of several B and A stars where strong flares may have been observed. Wang (1993) detected a flare on the A5/8V star BD+47 819 using photographic techniques. Miura et al. (2008) detected an intense X-ray flare on the A1 IV/V star HD 161084. The peak X-ray luminosity amounts to 10^{32} erg s^{-1} which is much larger than the X-ray luminosity of an ordinary late-type main-sequence star, indicating that the flare probably originates in the A-star itself rather than on a hidden late-type companion. Robrade & Schmitt (2011) detected a large X-ray flare in the Bp silicon star IQ Aur with temperatures up to $\approx 10^8$ K and a peak X-ray luminosity of $\approx 3 \times 10^{31}$ erg s^{-1}. The flare has a decay time of less than half an hour, originates from a rather compact structure and is accompanied by a significant metallicity increase. The X-ray properties of IQ Aur cannot be described by wind shocks only and require the presence of magnetic reconnection. Bhatt et al. (2014) found X-ray flares in two late-B stars belonging to the young open cluster NGC 869. Pye et al. (2015) found an X-ray flare in HD 31305 (A0) from the *XMM–Newton* serendipitous source catalogue. Flares on A stars are of particular interest because the very existence of flares, as well as active regions, indicates that current concepts of A-star atmospheres are not correct.

The magnetic properties of A stars may be divided into two groups: normal A stars and the Ap stars. The Ap stars constitute about 5 per cent of all A stars and are characterized by kilogauss dipole magnetic fields and patches of differing abundances, particularly overabundances of rare earth elements (Ryabchikova 2012). The anomalous abundances in Ap stars are thought to be a result of the interplay between gravitational settling and radiative acceleration of different atomic species (Michaud 1970). As a result, some elements diffuse upwards and others settle downwards provided there is little mixing. Mixing due to convection or meridional circulation destroys the natural segregation of elements due to diffusion that would otherwise occur. The presence of a large-scale

strong dipole magnetic field in Ap stars modifies the diffusion rate in accordance with the geometry of the field and is responsible for the abundance patches in Ap stars.

In spite of the fact that four Ap stars have been very well observed in SC mode in the *Kepler* data, no sign of flaring has been detected in these stars. On the other hand, the well-observed X-ray flare on IQ Aur (Robrade & Schmitt 2011) was detected. This star has a magnetic field of 1 kG (Wade et al. 2016). Whether or not the presence of a strong magnetic field inhibits flaring is therefore uncertain.

Normal A stars can have very weak global magnetic fields which have only been recently detected (Lignières et al. 2009; Petit et al. 2011). In recent years, weak magnetic fields have been detected in an increasing number of Am stars which are normal A stars with stronger metal lines (Blazère et al. 2015, 2016b; Blazère, Neiner & Petit 2016a). It is clear that weak global magnetic fields might well be common in A stars. The origin of the magnetic field is, however, a matter for debate.

It is well known that the convective cores in A and B stars are thought to act as vigorous dynamos, generating field strengths of several mega-Gauss (Featherstone et al. 2011). The magnetic flux tubes, however, are not sufficiently buoyant to rise to the surface. Hence, it is generally supposed that the strong surface magnetic fields in Ap stars are of fossil origin.

Although the subsurface convection zones in A stars are very thin, Cantiello & Braithwaite (2011) has suggested that dynamo action in these zones might generate a magnetic field. In this case, magnetic spots of size comparable to the local pressure scaleheight can manifest themselves as hot, bright spots.

A theory of dynamo action in radiative envelopes which involves differential rotation has been developed by Spruit (1999, 2002) and Maeder & Meynet (2004). In this theory, a magnetic instability in the toroidal field wound up by differential rotation replaces the role of convection in closing the field amplification loop in conventional dynamo theory. Zahn, Brun & Mathis (2007) has verified that an instability is generated, but concludes that a dynamo cannot be sustained by this effect. Arlt & Rüdiger (2011) found that feedback by the Lorentz force diminishes differential rotation and brings field growth to a halt in a few thousand years for intermediate-mass stars.

Although the presence of local magnetic fields of some strength are clearly present in A stars as shown by the occurrence of spots and flares, it seems that we still do not have an acceptable explanation for the generation of these fields.

12 DISCUSSION

We have shown that there is a strong tendency for flare stars of all spectral types to be the most rapidly rotating. We do not know if this is a direct effect of rotation on the flare-generating process or whether it is an indirect consequence of aging. The magnetically coupled winds in solar-like stars remove angular momentum and the rotation rate, and hence the efficiency of the stellar dynamo, drops as the star ages. The A stars are important because they do not have detectable stellar winds and therefore the incidence of stellar flares should not be correlated with age, but may still be correlated with rotation. Unfortunately, the number of flare A stars is presently too small to test this idea.

We tested the possibility that flare energies may be enhanced by differential rotation. For this purpose, we used the results of Balona & Abedigamba (2016) who determined the rotational shear in *Kepler* stars by measuring the spread in the rotation frequency. It turns out that there is no significant difference in rotational shear between flare and non-flare stars. This means that differential rotation has no significant effect on the flare energy.

We have shown that rotational variables occur among stars of all spectral types, though further observations of mid and early-B stars would improve the statistics. The evidence for star-spots in A stars is further supported by recent observations of the projected rotational velocity which shows the expected correlation with photometric period.

The distribution of star-spot sizes appears to approximate a log-normal distribution, as in the Sun. Observable star-spots seem to be at least three to six times larger than the largest sunspot observed, but this is likely to be an underestimate because we assume the spot to be single and completely dark. We show that there is a strong correlation between spot size and flare incidence in the sense that flare stars tend to be associated with spots which are about five times larger than those in non-flare stars.

The fact that star-spots and flares occur in A stars indicates that A stars, like cooler stars, have substantial localized magnetic fields. On the other hand A stars, unlike cooler stars, do not have a significant X-ray emission associated with a corona. The major difference between A stars and cooler stars is that cool stars have surface convection, whereas the surface convection zone in A stars is either absent or very thin. From this, we conclude that the presence of a corona is directly linked to the presence of surface convection. Physical considerations suggest that a magnetic field is also an essential component as the medium which transports heat from the photosphere to the upper atmosphere (Mandrini, Démoulin & Klimchuk 2000). However, it seems that convection is necessary for the corona to form.

The flaring rate, $N(E)$, was investigated as a function of flare energy, E, for different spectral classes. The resulting distributions can be described by a simple power law, $\mathrm{d}N/\mathrm{d}E \propto E^{\alpha}$, with $\alpha = -1.6$ to -1.7 for M–F stars but increasing to $\alpha = -1.3$ for A stars. The small number of A stars do not yet suggest that the difference is significant. We also investigated the distribution of flare duration. This also obeys a power law which is not significantly different for stars of different spectral types.

Finally, we discuss the problem of flares in A stars. These stars have flares with the highest energy. In part, this is explained by the fact that the detection limit increases from K stars to A stars owing to the increasing stellar luminosities. However, there is no reason why flares with energies similar to those in A stars should not exist in the cooler stars, since these flares would be the easiest to detect. The fact that flares of very high energy do not exist in K–M stars, but become more frequent for F and A stars shows that there is a real trend for stars with higher luminosities to have flares with higher energies. One explanation is that higher luminosity stars have larger radii and hence the active regions could have larger volumes, allowing a greater energy storage for dissipation during magnetic reconnection. However, the star-spot area is not much different for A stars and for cooler stars and the problem therefore remains unresolved.

Future prospects for progress in this field lie, to a large extent, in time series observations of low S/N and very high precision. It would be particularly important to extend the detection of flares and star-spots to B stars. The study of flares in stars with radiative envelopes allows the possibility of discriminating between the effects of convection and magnetism and also enables a much better study of the effect of rotation. To this end, the forthcoming TESS mission (Ricker et al. 2015) may provide a unique opportunity for such a study.

ACKNOWLEDGEMENTS

LAB wishes to thank the National Research Foundation of South Africa for financial support. The support of Czech Science Foundation is acknowledged (MŠ grant 15-02112S, MK grant P209/12/0103). MŠ and MK are further supported by institute research project RVO:67985815 to Astronomical Institute of Czech Academy of Sciences. We thank Petr Harmanec for many fruitful discussions on the topic and useful advice that influenced the research direction.

REFERENCES

Alfvén H., 1947, MNRAS, 107, 211
Arlt R., Rüdiger G., 2011, MNRAS, 412, 107
Aschwanden M. J., Tarbell T. D., Nightingale R. W., Schrijver C. J., Title A., Kankelborg C. C., Martens P., Warren H. P., 2000, ApJ, 535, 1047
Aschwanden M. J. et al., 2016, Space Sci. Rev., 198, 47
Balona L. A., 2012, MNRAS, 423, 3420
Balona L. A., 2013, MNRAS, 431, 2240
Balona L. A., 2015, MNRAS, 447, 2714
Balona L. A., 2016, MNRAS, 457, 3724
Balona L. A., Abedigamba O. P., 2016, MNRAS, 461, 497
Berghoefer T. W., Schmitt J. H. M. M., Danner R., Cassinelli J. P., 1997, A&A, 322, 167
Bhatt H., Pandey J. C., Singh K. P., Sagar R., Kumar B., 2014, J. Astrophys. Astron., 35, 39
Blazère A. et al., 2015, in Nagendra K. N., Bagnulo S., Centeno R., Jesús Martínez González M., eds, Proc. IAU Symp. 305, Polarimetry: From the Sun to Stars and Stellar Environments. Cambridge Univ. Press, Cambridge, p. 67
Blazère A., Neiner C., Petit P., 2016a, MNRAS, 459, L81
Blazère A. et al., 2016b, A&A, 586, A97
Bogdan T. J., Gilman P. A., Lerche I., Howard R., 1988, ApJ, 327, 451
Brown T. M., Latham D. W., Everett M. E., Esquerdo G. A., 2011, AJ, 142, 112
Candelaresi S., Hillier A., Maehara H., Brandenburg A., Shibata K., 2014, ApJ, 792, 67
Cantiello M., Braithwaite J., 2011, A&A, 534, A140
Choudhuri A. R., Schussler M., Dikpati M., 1995, A&A, 303, L29
Crosby N. B., Aschwanden M. J., Dennis B. R., 1993, Sol. Phys., 143, 275
De Moortel I., Browning P., 2015, Phil. Trans. R. Soc. A, 373, 20140269
De Rosa R. J. et al., 2011, MNRAS, 415, 854
Featherstone N. A., Browning M. K., Brun A. S., Toomre J., 2011, J. Phys. Conf. Ser., 271, 012068
Güdel M., Nazé Y., 2009, A&AR, 17, 309
Haisch B. M., Linsky J. L., Lampton M., Paresce F., Margon B., Stern R., 1977, ApJ, 213, L119
Heise J., Brinkman A. C., Schrijver J., Mewe R., Gronenschild E. H. B. M., den Boggende A. J. F., Grindlay J., 1975, ApJ, 202, L73
Hoge E. R., 1947, PASP, 59, 109
Huber D. et al., 2014, ApJS, 211, 2
Huensch M., Schmitt J. H. M. M., Voges W., 1998, A&AS, 132, 155
Johnstone C. P., Güdel M., 2015, A&A, 578, A129
Kallinger T., Matthews J. M., 2010, ApJ, 711, L35
Kowalski A. F., Hawley S. L., Wisniewski J. P., Osten R. A., Hilton E. J., Holtzman J. A., Schmidt S. J., Davenport J. R. A., 2013, ApJS, 207, 15
Küker M., Stix M., 2001, A&A, 366, 668
Lignières F., Petit P., Böhm T., Aurière M., 2009, A&A, 500, L41
Lovell B., 1963, Nature, 198, 228
McQuillan A., Mazeh T., Aigrain S., 2013, ApJ, 775, L11
McQuillan A., Mazeh T., Aigrain S., 2014, ApJS, 211, 24
Maeder A., Meynet G., 2004, A&A, 422, 225
Maehara H. et al., 2012, Nature, 485, 478
Maehara H., Shibayama T., Notsu Y., Notsu S., Honda S., Nogami D., Shibata K., 2016, preprint (arXiv:e-prints)
Mandrini C. H., Démoulin P., Klimchuk J. A., 2000, ApJ, 530, 999
Michaud G., 1970, ApJ, 160, 641
Miura J., Tsujimoto M., Tsuboi Y., Maeda Y., Sugawara Y., Koyama K., Yamauchi S., 2008, PASJ, 60, 49
Neff J. E., Simon T., 2008, ApJ, 685, 478
Nielsen M. B., Gizon L., Schunker H., Karoff C., 2013, A&A, 557, L10
Notsu Y. et al., 2013, ApJ, 771, 127
Noyes R. W., Hartmann L. W., Baliunas S. L., Duncan D. K., Vaughan A. H., 1984, ApJ, 279, 763
Pallavicini R., Golub L., Rosner R., Vaiana G. S., Ayres T., Linsky J. L., 1981, ApJ, 248, 279
Parker E. N., 1988, ApJ, 330, 474
Petit P. et al., 2011, A&A, 532, L13
Pye J. P., Rosen S., Fyfe D., Schröder A. C., 2015, A&A, 581, A28
Reinhold T., Reiners A., Basri G., 2013, A&A, 560, A4
Ricker G. R. et al., 2015, J. Astron. Telesc. Instrum. Syst., 1, 014003
Robrade J., Schmitt J. H. M. M., 2011, A&A, 531, A58
Ryabchikova T. A., 2012, in Zakharova P. E., Kuznetsov E. D., Ostrovskii A. B., Salii S. V., Sobolev A. M., Kholshevnikov K. V., Shustov B. M., eds, Physics of Space: the 41st Annual Student Scientific Conference. The Ural Federal University, p. 116
Samus N. N. et al., 2009, VizieR Online Data Catalog, 1, 2025
Schaefer B. E., 1989, ApJ, 337, 927
Schröder C., Schmitt J. H. M. M., 2007, A&A, 475, 677
Shibata K., 1999, Ap&SS, 264, 129
Shibata K., Magara T., 2011, Living Rev. Sol. Phys., 8, 6
Shibayama T. et al., 2013, ApJS, 209, 5
Shimizu T., 1995, PASJ, 47, 251
Smith J. C. et al., 2012, PASP, 124, 1000
Spruit H. C., 1999, A&A, 349, 189
Spruit H. C., 2002, A&A, 381, 923
Stumpe M. C. et al., 2012, PASP, 124, 985
Torres G., Andersen J., Giménez A., 2010, A&AR, 18, 67
Wade G. A. et al., 2016, MNRAS, 456, 2
Wang J., 1993, Inf. Bull. Var. Stars, 3836, 1
Wright N. J., Drake J. J., Mamajek E. E., Henry G. W., 2011, ApJ, 743, 48
Zahn J.-P., Brun A. S., Mathis S., 2007, A&A, 474, 145

This paper has been typeset from a TEX/LATEX file prepared by the author.